AIAA JOURNAL
Vol. 31, No. 4, April 1993

Quasiconical Free Interaction Between a Swept Shock and a Turbulent Boundary Layer

Frank K. Lu*
University of Texas at Arlington, Arlington, Texas 76019

Previous observations that fin-generated interactions are quasiconical in nature were further confirmed by surface pressure measurements spanning Mach 2.5–3.5, which encompassed unseparated through strongly separated interactions. For strongly separated interactions in which the shock wave is bifurcated into a λ-foot structure, the conical free interaction hypothesis was validated through an appropriate scaling of the far-field surface pressure distribution. The behavior of the λ-foot structure, such as the decrease of the slope of the separation shock with interaction strength, was explained by invoking the conical free interaction hypothesis. Through the conical free interaction hypothesis, it was further shown that the triple-shock intersection behaves in a complicated manner with changes in interaction strength.

Nomenclature

M	= Mach number
p	= pressure
p^*	= normalized pressure in conical free interaction, Eq. (4)
r	= distance measured from the virtual origin, Fig. 1
Re_θ	= Reynolds number based on momentum thickness
s	= distance measured from the fin apex, Fig. 1
(x, y, z)	= Cartesian coordinate system, Fig. 1
α	= fin angle, Fig. 1
β	= angle measured from incoming freestream direction centered at the virtual origin, Fig. 1
β^*	= normalized angle in conical free interaction, Eq. (3)
θ	= angle measured from incoming freestream direction centered at the fin apex, Fig. 1
ξ	= pressure ratio across a shock wave
ϕ	= azimuthal angle
ψ	= angle on the surface of a unit sphere
Subscripts	
b	= displacement surface at onset of flow separation
incip	= incipient
n	= normal to main shock
plat	= plateau
sep	= value at the separation line
ss	= separation shock
tp	= triple point
U	= upstream influence
0	= inviscid shock trace on test surface
1	= inviscid conditions of incoming freestream
2	= downstream inviscid conditions of main shock
3	= downstream inviscid conditions of separation shock
∞	= incoming freestream or incoming static value

Introduction

SWEPT shock wave, turbulent boundary-layer interactions remain a dauntingly complex problem in fluid mechanics today. Recent investigations have enhanced the understanding of such interactions[1,2] largely through parametric studies employing basic shock generator shapes such as fins, swept compression corners, etc. A shock generator extensively used in swept interaction studies is that of a sharp fin, depicted schematically in Fig. 1. This geometry is deceptively simple. An inviscid, attached shock solution is readily obtainable if the incidence angle α is small enough as is the case of all previously known investigations. Such a fin-generated, shock boundary-layer interaction exhibits all of the key features common to a family of semi-infinite, dimensionless interactions.[1] (Semi-infinite refers to the fact that when the shock generator dimensions are large enough, further increases in these dimensions do not change the interaction flowfield, whereas dimensionless means that the shock generator imposes no length scale on the interaction.) The simple inviscid solution and the presence of all the interaction features perhaps account for the prevalence of the fin configuration in basic research.

Early experimental observations showed that fin interactions are quasiconical in nature,[3] these observations being reinforced by subsequent analysis[4] and computations.[5] The flowfield upstream of the inviscid shock and also somewhat downstream appears to radiate from a "virtual" origin displaced from the fin apex as indicated in Fig. 1. This conical behavior from the virtual origin only exists beyond an inception zone near the fin leading edge as depicted in Fig. 2.[6] Hence, for surface features, instead of a Cartesian coordinate system, a polar coordinate system (r, β) centered at the virtual origin is appropriate whereas in the far field only the β angular coordinate suffices. Recent studies,[5,7] however, showed that the

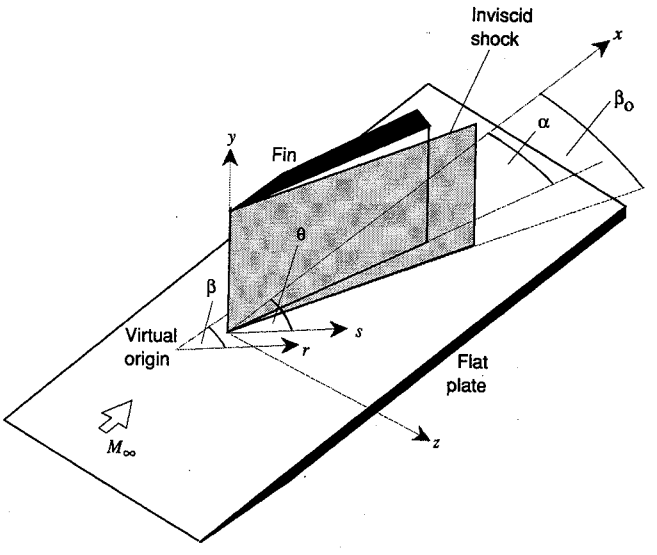

Fig. 1 Schematic of test geometry.

Received April 4, 1992; revision received Sept. 4, 1992; accepted for publication Sept. 10, 1992.

*Assistant Professor, Aerodynamics Research Center, Mechanical and Aerospace Engineering Department. Senior Member AIAA.

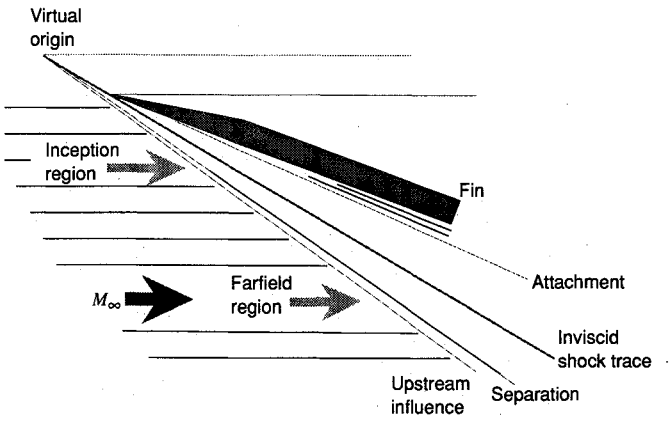

Fig. 2 Schematic showing key surface features of a separated interaction.

far-field skin friction and heat-transfer coefficients of separated interactions do not possess conical symmetry. The reason is that along a given ray from the virtual origin, i.e., with $\beta = \text{const}$, the surface streamline at the radial distance will have arrived there from the attachment line after traversing a shorter distance than a surface streamline at a farther distance away. Thus, experiments by Kim and Settles[7] and computations by Knight and Badekas[5] showed a steady rise of skin friction coefficient with r and a leveling off which occurs somewhat later than expected from inception length data obtained through surface flow visualization.[6] The basis for this nonconical behavior of properties involving derivatives of pressure, velocity, or temperature is explained in Courant and Friedrichs.[8] For present purposes, the term quasiconical interaction can be taken to mean that near the fin leading edge there is a fully three-dimensional inception zone and that basic flow properties in the far field possess conical behavior but not "higher-order" properties.

The early investigations relied heavily on surface flow visualization which provides a convenient way of determining the surface "footprint" of the interaction.[9] Figure 2 depicts schematically features observed in the surface visualization trace of a separated interaction, incipient separation being assumed to occur when surface streaks from upstream of the interaction just begin to coalesce. The shock strength $\xi_{12} = p_2/p_1$ at incipient separation, to first order, is found to be independent of Mach and Reynolds number and the incipient value of α is given by the correlation.[10]

$$\alpha_{\text{incip}} = 0.3/M_\infty \text{ rad} \approx 17.2/M_\infty \text{ deg} \qquad (1)$$

This corresponds to $\xi_{12\text{incip}} = 1.5$–$1.6$. A detailed analysis by Zheltovodov et al.[11] showed that $\xi_{12\text{incip}}$ decreases from 1.8 to 1.5 as Re_θ increases from 10^3 to 10^5, i.e., α_{incip} decreases with increase in Reynolds number.[12] (A more recent analysis that showed the same behavior was performed by Dou and Deng.[13]) The onset of the interaction is marked by a deflection of the incoming surface streaks and is indicated in Fig. 2 as the upstream influence line. The separated zone is marked by a curved "feather" pattern from the separation line in front to the attachment line near the junction of the fin and flat plate. The surface flow between the attachment line and the junction is roughly parallel to the fin. Above a certain shock strength, an enigmatic "secondary separation" exists within the primary separated flow.[1,2]

Subsequently, flow visualizations[14–17] revealed features within the flowfield that can be tied to previous observations of surface phenomena. An example of an image obtained by the lightscreen technique is shown in Fig. 3a with an accompanying diagram in Fig. 3b. (The lightscreen technique is briefly summarized in the next section.) The crossflow direction is from right to left. Because of limitations in the experiment[14] (see the following section), the view in Fig. 3a is nearly orthogonal to the main shock. Spurious artifacts in Fig. 3a include the bright reflection off the fin surface and a faint curved feature on the upper left due to imperfections in the optical system.

As indicated in Fig. 3b, the conical far-field features are appropriately represented on the surface of a unit sphere. The features on a spherical surface can be cast onto a plane using cartographic projections and an azimuthal equidistant projection is chosen for accuracy. In this projection, rays emanating from the center of the sphere are intercepted by a plane orthogonal to a given radial, datum line that is chosen as the inviscid shock trace. Angles measured on the spherical surface are denoted by ψ whereas the coordinates of structural features are given by the latitudinal and longitudinal angles β and ϕ.

At Mach 3.44, the interaction induced by an $\alpha = 15$-deg fin is highly separated. A most distinct feature in Fig. 3a that is associated with the separated flow is the λ-foot structure in which the main, freestream shock bifurcates into a forward, separation shock and a rear, internal shock. The visualizations reveal that the separated boundary layer thickens while pathlines obtained through computer simulations[18] show that the separated flow consists of a highly swept vortical structure. The separation shock appears straight in flow visualization and its angle is ψ_{ss}. This shock is induced by a flow deflection of ψ_b due to thickening of the displacement surface.

The inviscid flow above the boundary layer is processed by the separation and rear shocks whose combined strength is less than that of the main shock. Thus, toward the rear of the λ foot, a slip surface exists between this flow and the less energetic flow down-

a) Photograph

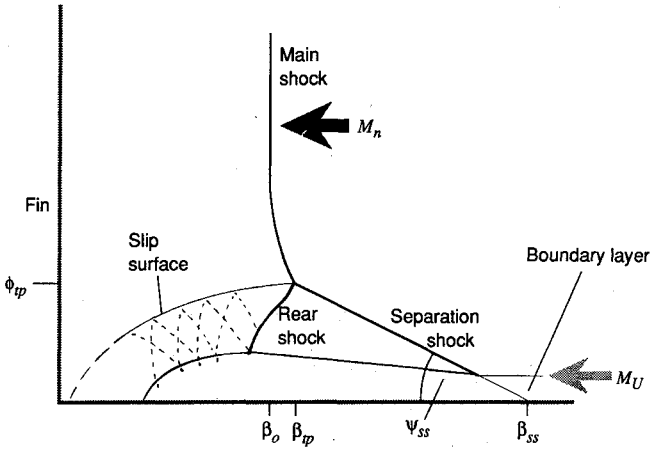

b) Diagram

Fig. 3 Lightscreen image of a separated interaction ($M_\infty = 3.44$, $\alpha = 15$ deg).

stream of the main shock. The flow in the channel between the boundary layer and the slip surface is turned toward the test surface by a series of compressions and expansions (shown as dotted lines) and possibly by a terminal shock.[16] According to Alvi and Settles,[16] wave focusing may give rise to "shocklets" in this curved channel. This channel flow impinges on the test surface, and, in strongly separated interactions, the surface pressure at flow attachment exceeds the downstream inviscid value. However, interaction details at the fin junction are still poorly understood and the slip surface here is drawn with dashed lines in Fig. 3b. For further discussion on the evolution of the flowfield with interaction strength, including the appearance of secondary separation, see Ref. 16.

The preceding review highlights only parts of the tremendous progress made recently in understanding shock wave, boundary-layer interactions that are relevant to the present work. To further reinforce previous observations in the supersonic range, this paper presents and analyzes surface pressure measurements to support the conical free interaction hypothesis. The conical free interaction is then used to interpret hitherto unexplained behavior of the separation shock and the triple-shock intersection with changes in the interaction strength. Before discussing the results, brief details of surface pressure and lightscreen experiments will be given. (Preliminary lightscreen results were reported in Ref. 14.)

Experimental Methods

The supersonic wind tunnel of Pennsylvania State University's Gas Dynamics Laboratory was used to obtain the data presented in this paper. Details of the tunnel, test models, test conditions, and experimental techniques can be found in Lu[19] and were previously reported as well.[6,20] Briefly, the tests were performed at Mach numbers of 2.47, 2.95, and 3.44, with unit Reynolds numbers of 54×10^6 m^{-1}, 59×10^6 m^{-1}, and 64×10^6 m^{-1}, respectively. The wind tunnel had a test section 150 mm wide, 165 mm high, and 610 mm long. A 500-mm-long flat plate with a sharp leading edge spanned the test section and served as the test surface. A two-dimensional, turbulent, equilibrium, adiabatic boundary layer developed naturally on this flat plate. The undisturbed boundary layer at the tip of the fin was about 3.3 mm thick for the three Mach numbers. The fin tip was located 216 mm from the flat plate's leading edge and 26 mm from one of the tunnel's walls. The fin was 100 mm high, 127 mm long, and 10.3 mm thick and was high enough to ensure that a semi-infinite interaction was obtained.[1] The fin was mounted perpendicularly and tightly on the flat plate and could be swivelled by a pneumatic actuator which, consequently, allowed the experiments to be performed with relative ease. The fin angle of attack ranged from 4 deg to the stall limit of about 22 deg. A total of 21 fin angle and Mach number combinations were tested and these combinations ranged from unseparated to strongly separated cases.

For surface pressure measurements, 0.508-mm-diam taps were drilled onto the flat plate. The small diameter ensured adequate spatial resolution by allowing the pressure taps to be densely packed along each row. The taps were laid out along circular arcs centered at the fin tip. This layout exploited the quasiconical symmetry of the interaction and was previously used by Zubin and Ostapenko.[21] There were five rows of taps at r = 31.8, 50.8, 76.2, 101.6, and 127.0 mm with θ ranging from 7.5 to 61 deg. Ninety-six taps were available and these were connected by pressure tubing to a 96-port, dual-channel Scanivalve™ pressure scanning system. The interaction pressures, a reference pressure, and other data for computing the test conditions were acquired through a microcomputer-based data acquisition system; this computer also controlled the Scanivalves. Although 96 taps were connected to the pressure scanning system, not all of the measurements were useful. This is because at certain fin angles, some taps were either covered by the fin or were in the leeward side. Also, at high fin angles, some of the pressure data at large (r, θ) were affected by tunnel wall interference. Finally, although the pressure taps were laid out in arcs centered at the fin tip, a simple transformation can be performed to obtain the surface pressure distribution in the (r, β) coordinate system once the distance from the fin tip to the virtual origin is known.[6]

For lightscreen experiments, compressed air was stored without passing through the normal drying equipment and therefore retained some moisture. With a dewpoint of -14 ± 2°C, moisture contributed to an error of less than 1% to static pressure measurements for the present Mach number range.[22] This residual amount of moisture allowed adequate light to be scattered and photographed. (Under normal circumstances, the tunnel dewpoint was about -22 ± 2°C.) A smaller test matrix than surface pressure measurements was used for the visualizations, these being with fins set at $\alpha = 7$, 10, 15, and 18 deg except that the 18-deg case at Mach 2.47 caused tunnel stall and was thus not tested. The lightscreen technique is recently reviewed by Philbert et al.[23] and is described in great detail by Snow and Morris.[24] Its discussion is thus omitted for brevity. In the present implementation, a 4-W argon-ion laser beam was spread into a 1.2-mm-thick sheet by a cylindrical lens. This sheet passed about 5 mm to the rear of the fin to reduce stray reflections from the test model even though the model was painted matt black. This requirement, unfortunately, prevented the light sheet from being incident normally to the freestream shock due to limited optical access. The light sheet was photographed using a 35-mm camera with a macrofocusing zoom lens. A reference photograph of 2.54-mm square grids that coincided with the light sheet was taken to enable flow structures in the actual images to be corrected to the azimuthal equidistant projection.

Results and Discussion

Quasiconical Symmetry

Examples of two surface pressure distributions are displayed in Fig. 4. As reviewed earlier, incipient separation corresponds to ξ_{12}

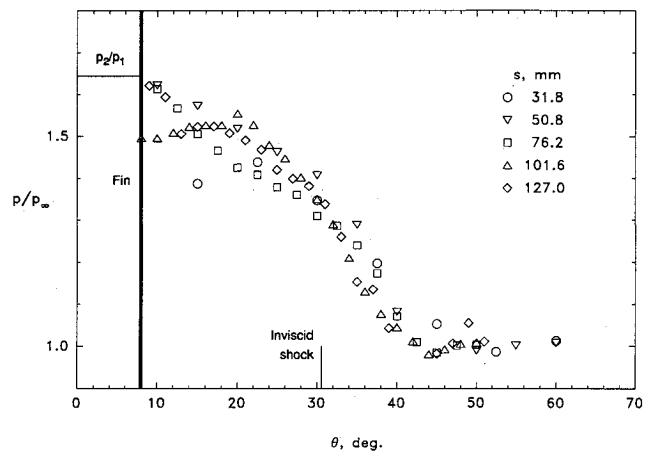

a) $M_\infty = 2.47$, $\alpha = 8$ deg

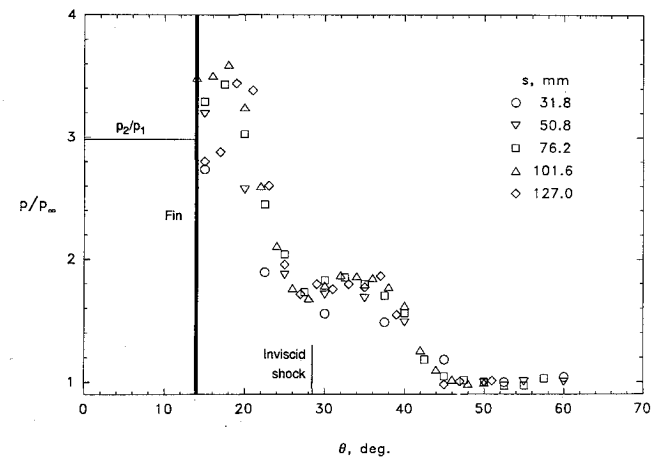

b) $M_\infty = 3.44$, $\alpha = 14$ deg

Fig. 4 Examples of surface pressure distribution of fin interaction.

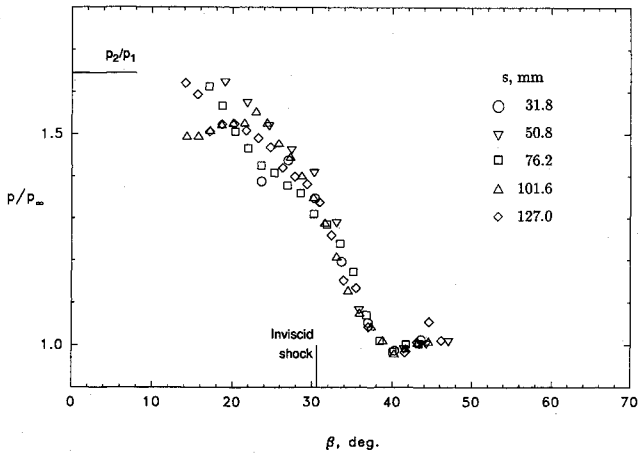

a) $M_\infty = 2.47$, $\alpha = 8$ deg

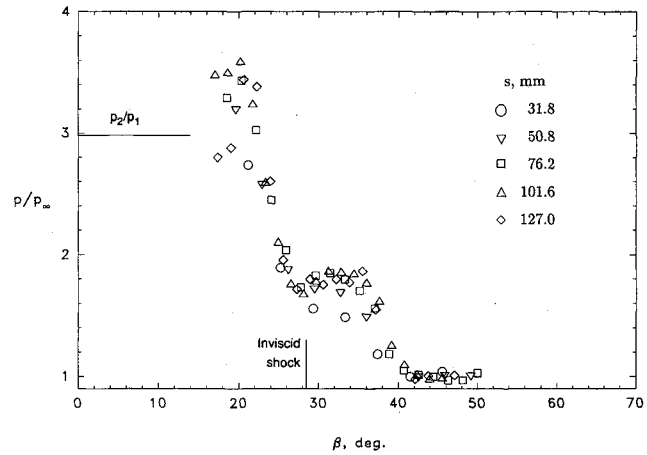

b) $M_\infty = 3.44$, $\alpha = 14$ deg

Fig. 5 Examples of surface pressure distribution with coordinates corrected to the virtual origin.

in the 1.5–1.8 range and, therefore, Fig. 4a displays the surface pressure distribution of an interaction that is around incipient separation. The surface pressure distribution shows a monotonic rise up to approximately the inviscid level. Further, the first row of data at $s = 31.8$ mm shows that the pressure does not rise to the inviscid level, this being indicative of an interaction that is not fully developed. Turning to Fig. 4b, the surface pressure distribution is characteristic of a separated interaction showing a distinctive plateau in the separated zone at between 30 and 38 deg and a dip around the inviscid shock. Near to the fin junction, an "overshoot" occurs with the surface pressure exceeding the inviscid downstream value. The plateau and dip have been commonly attributed to a highly swept vortical structure in separated interactions.[18] The data at $s = 31.8$ and 50.8 mm are also evidently in the inception zone and this nonconical behavior will be more vividly seen next.

In both examples, it appears that the (s, θ) coordinate system essentially captures the conical nature of the interaction if s is large since the distributions at different rows collapse fairly well. This is especially true of the weaker interaction shown in Fig. 4a and it may even lead one to conclude that the interaction possesses a negligibly small inception zone. In fact, in weak, unseparated interactions that are highly swept, the opening angle from the fin apex $(\theta - \theta_0)$ is virtually equal with that from the virtual origin $(\beta - \beta_0)$ despite these interactions having large inception zones.[6] To confirm the quasiconical nature of the surface pressure distribution, the pressure tap locations were corrected to the (r, β) coordinate system using inception length data reported previously.[6] The corrected distributions are displayed in Figs. 5a and 5b. In these figures, there is a slight displacement of the r coordinate from the constant radii in the (s, θ) coordinate system. This error is extremely slight and is unimportant in the case of conical symmetry. A comparison of Figs. 5a and 5b with Figs. 4a and 4b shows an improvement in the collapse of the pressure distribution for the outermost rows in the region approximately upstream of the inviscid shock location, reinforcing previous observations of conical symmetry deduced from surface pressures measured along streamwise rows.[3] The inception zone data obviously do not collapse with those of the far field as is especially manifest in Fig. 5b.

The upstream influence angle can also be estimated from the far-field surface pressure distribution. For the two cases shown in Figs. 5a and 5b, $\beta_U = 38$ and 40 deg, respectively. These values compare favorably with directly measured values from surface flow visualization of 38.5 and 39.6 deg, respectively, or with those obtained from the relation[20]

$$\Delta\beta_U = 2.2\Delta\beta_0 - 0.027\Delta\beta_0^2 \qquad (2)$$

which yields $\beta_U = 37.4$ and 38.9 deg, respectively. Hence, even though the upstream influence has traditionally been defined in terms of a first detectable increase in pressure, the close agreement between surface pressure measurement and surface flow visualization confirms the viability of the latter technique[25] and its application has been widespread due to its convenience.[3,6,20] However, it is worthwhile to note that both surface pressure measurement and surface flow visualization are not able to capture time-dependent details of the upstream influence.[26]

Conical Free Interaction

A consequence of "conical free interaction,"[27] analogous to the two-dimensional concept,[28,29] is that the surface pressure distribution upstream of the main shock should exhibit a universal form. The surface pressure distributions of strongly separated, swept interactions all possess the characteristic plateau and dip mentioned in the Introduction. But the angular extent of the interaction or the magnitude of the plateau pressure can be very different. Therefore, a normalization procedure must be performed first which, if the conical free interaction hypothesis is valid, should result in a universal pressure distribution. Hayes[30] previously showed that $(p - p_\infty)/(p_{plat} - p_\infty)$ scales with $(z - z_{sep})/(z_U - z_{sep})$ which is similar to that used by Zukoski[31] for demonstrating two-dimensional free interaction. In the spherical framework of conical interactions where only angles are needed, the abscissa can be simplified to

$$\beta^* = (\beta - \beta_0)/(\beta_U - \beta_0) \qquad (3)$$

Such a scaling normalizes all circular segments, regardless of their original sizes, to stretch from $\beta^* = 1$ at the upstream influence to

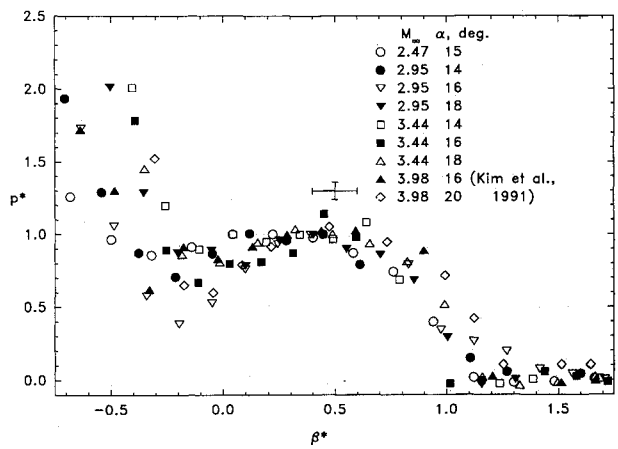

Fig. 6 Conical free interaction in strongly separated, swept interactions.

$\beta^*=0$ at the inviscid freestream shock trace. The next step is to scale the surface pressure. The parameter chosen is[30,31]

$$p^* = (p - p_\infty)/(p_{plat} - p_\infty) \tag{4}$$

If there is a universal pressure distribution, then a plot of the far-field p^* data against β^* should show collapse. The far-field data obtained from the present experiments and those of Kim et al.[32] are plotted in Fig 6. In the normalization procedure, an average error of about $\pm 10\%$ was incurred in β^* and about $\pm 6\%$ was incurred in p^* in the plateau region as marked by a cross in Fig. 6. Errors were larger toward the upstream influence. Within the experimental error, it can be seen that the data collapse fairly well into a universal distribution, reinforcing the conical free interaction hypothesis. It can be noted that only strongly separated cases show such similarity, namely, where $\xi_{12} \gtrsim 2.3$. Interestingly, this limit corresponds to the onset of secondary separation.[1,15,33] In addition, the plateau "hump" appears at $\beta^* \approx 0.5$, that is, it is located at the bisection of the main shock trace and the upstream influence.

Separation Shock

A further demonstration of conical free interaction can be obtained by examining the mean separation structure at the upstream influence. From flow visualization images,[14,16] the forward separation shock can be extrapolated through the boundary layer to impinge upon the test surface. In the conical far field, this impingement location has an angular coordinate β_{ss}. Since, in two-dimensional separated interactions, a compression system originates from the upstream influence and coalesces into the separation shock,[29] it is natural to determine quantitatively if a similar situation also occurs for swept interactions. This is illustrated by Fig. 7, which plots β_{ss} as closed symbols and β_U obtained previously[20] as open symbols. Equation (2) is also plotted as solid lines. It is clear from this plot that

$$\beta_U = \beta_{ss} \tag{5}$$

within the data scatter and that the mean separation shock trace on the test surface bears an intimate relationship with the upstream influence.[26] Lightscreen images for the $M_\infty = 2.47$ cases showed either unseparated or weakly separated flows. In the latter case, the λ-foot structure was small and difficult to quantify. Therefore, in the discussions, no Mach 2.47 cases will be included.

It is well known that in separated, two-dimensional interactions, the separation shock angle depends on the incoming Mach number and the deflection of the displacement surface of the separation bubble,[28,29] corresponding to the incipient separation shock strength discussed earlier. The displacement surface possesses a deflection that is roughly constant in slope in the 8–12-deg range so that an increase in the Mach number results in a decrease of the separation shock angle. A similar phenomenon of a decrease in

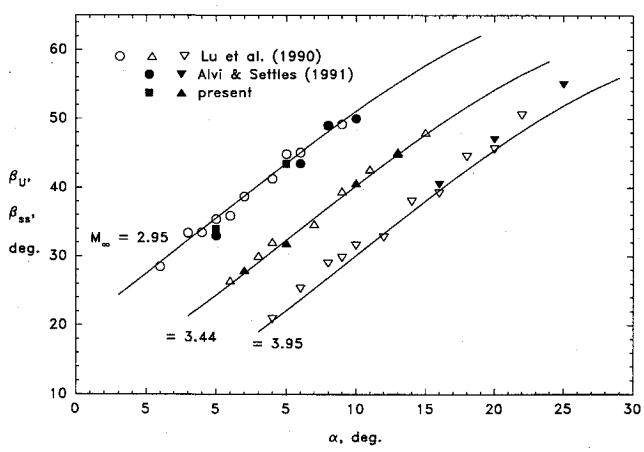

Fig. 7 Comparison of β_{ss} with β_U.

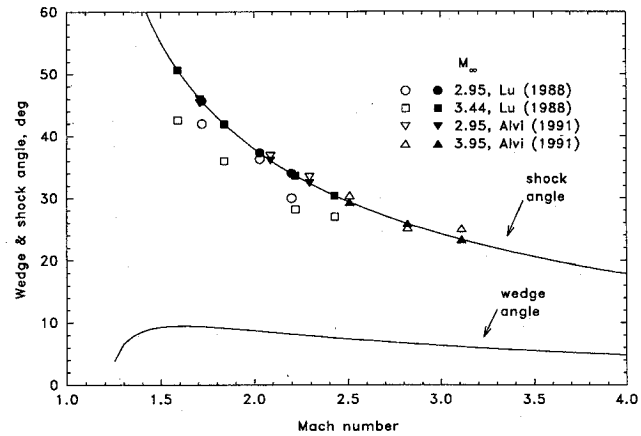

Fig. 8 Separation shock angle.

separation shock angle with increase in *normal* Mach number M_n and roughly constant deflection angle is found in conical interactions.[11,14–16] In fact Alvi and Settles[15] found that the separation shock angle ψ_{ss} can be correlated against M_n. This observation notwithstanding, since the separation shock impinges the boundary layer at the upstream influence, it appears that a more appropriate Mach number for correlating ψ_{ss} based on the conical free interaction hypothesis may be the Mach number normal to the upstream influence line[11,34]

$$M_U = M_\infty \sin\beta_U \tag{6}$$

Oblique shock theory yields a relationship between the separation shock angle ψ_{ss} and M_U as

$$\psi_{ss} = \arcsin(\Pi_{ss}/M_U) \tag{7}$$

where

$$\Pi_{ss} = \sqrt{\frac{(\gamma+1)\xi_{13} + (\gamma-1)}{2\gamma}} \tag{8}$$

is a pressure function with $\xi_{13} = p_3/p_1$ being the pressure ratio across the separation shock. Moreover, it is a physically plausible assumption that $\xi_{13} = 1.6$, i.e., the separation shock is of such strength that it just induces the incoming boundary layer to separate, similar to the two-dimensional situation. The inviscid solution of Eq. (7) with this assumed value of ξ_{13} is plotted in Fig. 8. The figure also shows the wedge angle ψ_b which approximates the actual deflection of the boundary-layer displacement surface at the interaction onset needed to induce the separation shock and experimental results which will be discussed later. A sensitivity check was made using values of p_3/p_1 from 1.4 to 1.8, covering the range of incipient separation values, and it was found that the shock or wedge angles were not far different from those displayed in Fig. 8, certainly within experimental error of 1 or 2 deg for the shock angle.

Separation shock angles[14,16] are plotted in Fig. 8 against M_U as open symbols whereas those predicted using oblique shock theory are shown as closed symbols. Error bars have been deleted from Fig. 8 to reduce clutter. The original data showed that β_U could be estimated to an accuracy of about 0.5 deg for strong interactions such as those presented here.[19] This error and the error in determining M_∞ contributed to an error bar of ± 0.1 to the estimate of M_U. An error bar of less than ± 2 deg to the estimate of ψ_{ss} is obtained from Alvi and Settles' diagrams.[16] The present estimate of ψ_{ss} has an error of as much as ± 5 deg, this larger error compared to Alvi and Settles'[16] data being due to the aforementioned limited optical access. Alvi and Settles'[16] data agree remarkably well with those from calculations but the present data show larger disagree-

ment. Clearly the analysis shows that the physical process inducing separation for a broad range of supersonic swept interactions is the same, namely, that separation is induced by an oblique shock which causes the inviscid pressure to rise by about 1.6. The analysis also shows that the wedge angle necessary to induce separation is about 8 deg for a wide range of supersonic Mach numbers, confirming experimental observations. Further, the present analysis reveals that although ψ_{ss} correlates well with M_n, a physically more meaningful interpretation, using the conical free interaction concept, is that the separation shock is a weak shock that just induces the boundary layer to separate. The analysis puts on proper physical grounds the observation that the separation shock angle decreases with increasing interaction strength. This is required if the pressure rise across the separation shock is constant (for given Re_θ), this constant pressure being once again a universal consequence of free interaction. As an afterthought, previous observations[11,30,33] have found similarities between certain features in the surface pressure distribution of strongly separated, swept interactions and those in strongly separated, two-dimensional interactions. It may be that the link between these two classes of interactions is that the shock-induced separation is of a universal nature and that the crossflow normal to the upstream influence line in the swept interaction case is of secondary importance.

Triple-Shock Intersection

The triple-shock problem arising from shock reflections remains one of some interest.[35] It is not completely understood in two-dimensional flows and is much less so in three-dimensional ones. In this section, an approximate analysis will be given of the triple-shock intersection in swept interactions that provides physical insights to experimentally observed behavior. In two-dimensional Mach reflections, situations arise in which the "Mach stem" is curved due to the requirement that the pressure across the slip line must be equal. Analogously, the same phenomenon occurs in the triple-shock intersection in swept shock, boundary-layer interactions in which case the main shock is equivalent to the Mach stem, see Fig. 3.The main shock curves forward in all of the cases examined with the curvature decreasing as the interaction strengthens. This can be illustrated by a plot of β_{tp} against α in Fig. 9. A consequence of the main shock curvature is that the rear shock is also curved.[35] Therefore, the flow leaving the λ-shock system is nonuniform, resulting in the presence of waves on either side of the slip surface. These waves are particularly noticeable in highly sensitive interferograms.[17]

Regardless of the preceding observations, in the present analysis, the main shock is assumed to remain straight for simplicity. The separation shock, therefore, intersects the main shock not at β_{tp} but at β_0 and its azimuthal angle is ϕ_{tp}, see Fig. 3. Conical free interaction allows an estimate of ϕ_{tp} to be obtained. On a unit sphere, trigonometry yields

$$\phi_{tp} = \arctan\left[\sin\left(\beta_U - \beta_0\right)\tan\psi_{ss}\right] \tag{9}$$

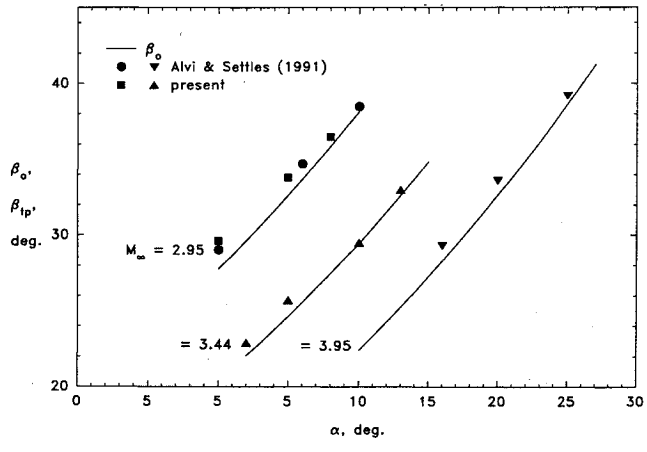

Fig. 9 Trace of the triple-shock intersection on the test surface.

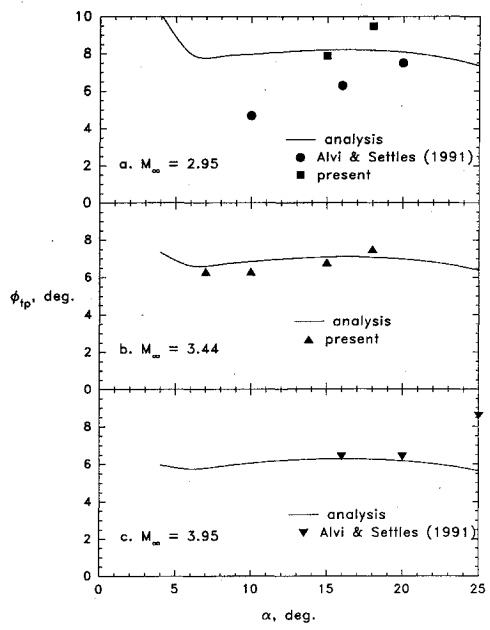

Fig. 10 Azimuthal angle of triple-shock intersection.

where ψ_{ss} is given by Eq. (7). Equation (9) is accurate only when the main shock exhibits small curvature whereas it further shows that ϕ_{tp} is in fact a complicated function of both M_n and M_U through $\beta_U - \beta_0$ and ψ_{ss}. Therefore, instead of attempting to discover possible scaling laws for ϕ_{tp}, a comparison with experimental data is given in terms of α in Fig. 10. [The predicted values make use of β_U obtained from Eq. (2).] As shown in Fig. 10, Eq. (9) predicts an increase in ϕ_{tp} with a decrease of α, this arising from the larger values of ψ_{ss} for weakly separated interactions, see Fig. 8. These weaker interactions also possess highly curved main shocks and, therefore, the analysis is not expected to be valid. Throughout a large range of α where the analysis is expected to be valid, it can be seen that ϕ_{tp} is a weak function of interaction strength at *each* incoming freestream Mach number. Excluding the spurious low-α region, the analysis shows that ϕ_{tp} increases slightly with α and then decreases. Also, the analysis shows that ϕ_{tp} decreases with increasing incoming freestream Mach number. It appears that the angular extent of the interaction's footprint grows very rapidly with increasing interaction strength either through increase of M_∞ or α but the azimuthal extent of the interaction remains fairly small and may even decrease, giving rise to an extremely flattened interaction. Conversely, at a given Mach number and with an approximately constant value of ϕ_{tp}, the free interaction result that ξ_{13} is constant requires that ψ_{ss} has to decrease with increasing interaction strength, resulting in an increase of β_{ss} or, equivalently, β_U.[20] Moreover, the rate of decrease of ψ_{ss} with M_U slows down as M_n gets large and this is also reflected in the decrease in the rate of growth of β_U, which is thought to tend to β_0 for very strong interactions.[20]

Turning next to the measured values of ϕ_{tp}, the triple-shock intersection from the present test matrix at Mach 2.95 and α of 7 and 10 deg could not be determined with confidence and is not shown in the figure. Overall, the analysis shows that for stronger interactions, the predictions follow the experimental results fairly well except for the Mach 2.95 data of Alvi and Settles.[16] For the Mach 3.95 comparison, the strongest case of Alvi and Settles[16] may be subjected to tunnel sidewall interference which would distort the interaction somewhat and which would cause ϕ_{tp} to be larger than expected.

Conclusions

Surface pressure data measured in a polar coordinate system confirmed previous observations that highly swept, semi-infinite, dimensionless interactions are quasiconical in nature. In the far

field, strongly separated interactions which possess a λ-foot shock structure are freely interacting in that the shock strength to induce separation is approximately constant and is, in fact, the incipient separation value. This fact is manifested by the decrease in the slope of the separation shock with increasing shock strength. The mean separation shock was found to impinge the test surface at the upstream influence line. In the complex viscous-inviscid interaction set up at the upstream influence, a "local" analysis can account for the decrease of the separation shock with increasing shock strength. Finally, the conical free interaction forces a complicated behavior of the triple-shock intersection with changes in interaction strength.

Acknowledgments

The experiments were supported by Air Force Office of Scientific Research Grant 86-0092 monitored by Len Sakell and by NASA Ames through Grant NCA2-1R589-502 monitored by C. C. Horstman. These funding sources are acknowledged with gratitude. The author wishes to express his deep appreciation to Gary S. Settles who supervised his doctoral research which produced the data reported here.

References

[1]Settles, G. S., and Dolling, D. S., "Swept Shock Wave/Boundary-Layer Interactions," *Tactical Missile Aerodynamics*, edited by M. J. Hemsch and J. N. Nielsen, Vol. 104, Progress in Astronautics and Aeronautics, AIAA, Washington, DC, 1986, pp. 297–379.

[2]Settles, G. S., and Dolling, D. S., "Swept Shock/Boundary-Layer Interactions—Tutorial and Update," AIAA Paper 90-0375, Jan. 1990.

[3]Settles, G. S., and Lu, F. K., "Conical Similarity of Shock/Boundary-Layer Interactions Generated by Swept and Unswept Fins," *AIAA Journal*, Vol. 23, No. 7, 1985, pp. 1021–1027.

[4]Inger, G. R., "Spanwise Propagation of Upstream Influence in Conical Swept Shock Boundary-Layer Interactions," *AIAA Journal*, Vol. 25, No. 2, 1987, pp. 287–293.

[5]Knight, D. D., and Badekas, D., "On the Quasi-Conical Flowfield Structure of the Swept Shock Wave-Turbulent Boundary Layer Interaction," AIAA Paper 91-1759, June 1991.

[6]Lu, F. K., and Settles, G. S., "Inception Length to a Fully-Developed Fin-Generated Shock Wave Boundary-Layer Interaction," *AIAA Journal*, Vol. 29, No. 5, 1991, pp. 758–762.

[7]Kim, K.-S., and Settles, G. S., "Skin Friction Measurements by Laser Interferometry in Swept Shock/Boundary-Layer Interactions," *AIAA Journal*, Vol. 28, No. 1, 1990, pp. 133–139.

[8]Courant, R., and Friedrichs, K. O., *Supersonic Flow and Shock Waves*, Springer-Verlag, New York, 1976, pp. 406–416.

[9]Lu, F. K., and Settles, G. S., "Color Surface-Flow Visualization of Fin-Generated Shock-Wave Boundary-Layer Interactions," *Experiments in Fluids*, Vol. 8, No. 6, 1990, pp. 352–354.

[10]Korkegi, R. H., "A Simple Correlation for Incipient Turbulent Boundary-Layer Separation Due to a Skewed Shock Wave," *AIAA Journal*, Vol. 11, No. 11, 1973, pp. 1578–1579.

[11]Zheltovodov, A. A., Maksimov, A. I., and Shilein, E. K., "Development of Turbulent Separated Flows in the Vicinity of Swept Shock Waves," *The Interactions of Complex 3-D Flows*, edited by A. M. Kharitonov, USSR Academy of Sciences, Inst. of Theoretical and Applied Mechanics, Novosibirsk, 1987, pp. 67–91.

[12]Goldberg, T. J., "Three-Dimensional Separation for Interaction of Shock Waves with Turbulent Boundary Layers," *AIAA Journal*, Vol. 11, No. 11, 1973, pp. 1573–1575.

[13]Dou, H., and Deng, X., "Prediction for the Incipient Separation of Fin-Generated Three-Dimensional Shock Wave Turbulent Boundary Layer Interactions," *Acta Aerodynamica Sinica*, Vol. 10, No. 1, 1992, pp. 45–52 (in Chinese).

[14]Lu, F. K., and Settles, G. S., "Structure of Fin-Shock/Boundary-Layer Interactions by Laser Light-Screen Visualization," AIAA Paper 88-3801, July 1988.

[15]Alvi, F. S., and Settles, G. S., "Structure of Swept Shock Wave/Boundary-Layer Interactions Using Conical Shadowgraphy," AIAA Paper 90-1644, June 1990.

[16]Alvi, F. S., and Settles, G. S., "A Physical Model of the Swept Shock/Boundary-Layer Interaction Flowfield," AIAA Paper 91-1768, June 1991.

[17]Hsu, J. C., and Settles, G. S., "Holographic Flowfield Density Measurements in Swept Shock Wave/Boundary-Layer Interactions," AIAA Paper 92-0746, Jan. 1992.

[18]Knight, D. D., Horstman, C. C., Shapey, B., and Bogdonoff, S. M., "Structure of Supersonic Turbulent Flow Past a Sharp Fin," *AIAA Journal*, Vol. 25, No. 11, 1987, pp. 1331–1337.

[19]Lu, F. K., "Fin-Generated Shock-Wave Boundary-Layer Interactions," Ph.D. Dissertation, Pennsylvania State Univ., University Park, PA, May 1988.

[20]Lu, F. K., Settles, G. S., and Horstman, C. C., "Mach Number Effects on Conical Surface Features of Swept Shock-Wave/Boundary-Layer Interactions," *AIAA Journal*, Vol. 28, No. 1, 1990, pp. 91–97.

[21]Zubin, M. A., and Ostapenko, N. A., "Structure of Flow in the Separation Region Resulting from Interaction of a Normal Shock Wave with a Boundary Layer in a Corner," *Izvestiya Akademii Nauk SSSR, Mekhanika Zhidkosti i Gaza*, Vol. 14, No. 3, 1979, pp. 51–58.

[22]Wegener, P. P., and Mack, L. M., "Condensation in Supersonic and Hypersonic Wind Tunnels," *Advances in Applied Mechanics*, Vol. V, 1958, pp. 307–407.

[23]Philbert, M., Surget, J., and Véret, C., "Light Sheet Technique," *Handbook of Flow Visualization*, edited by W.-J. Yang, Hemisphere, New York, 1989, pp. 211–217.

[24]Snow, W. L., and Morris, O. A., "Investigation of Light Source and Scattering Medium Related to Vapor-Screen Flow Visualization in a Supersonic Wind Tunnel," NASA TM-86290, 1984.

[25]Settles, G. S., and Bogdonoff, S. M., "Scaling of Two- and Three-Dimensional Shock/Turbulent Boundary-Layer Interactions at Compression Corners," *AIAA Journal*, Vol. 20, No. 6, 1982, pp. 782–789.

[26]Dolling, D. S., and Rodi, P. E., "Upstream Influence and Separation Scales in Fin-Induced Shock Turbulent Boundary-Layer Interaction," *Journal of Spacecraft and Rockets*, Vol. 25, No. 2, 1988, pp. 102–108.

[27]Settles, G. S., and Kimmel, R. L., "Similarity of Quasiconical Shock Wave/Turbuluent Boundary-Layer Interactions," *AIAA Journal*, Vol. 24, No. 1, 1986, pp. 47–53.

[28]Chapman, D. R., Kuehn, D. M., and Larson, H. K., "Investigation of Separated Flows in Supersonic and Subsonic Streams with Emphasis on the Effect of Transition," NACA Rept. 1356, 1958.

[29]Délery, J., and Marvin, J. G., "Shock-Wave Boundary Layer Interactions," AGARD-AG-280, 1986.

[30]Hayes, J. R., "Prediction Techniques for the Characteristics of Fin Generated Three Dimensional Shock Wave Turbulent Boundary Layer Interactions," Air Force Flight Dynamics Lab., AFFDL-TR-77-10, Wright-Patterson AFB, OH, 1977.

[31]Zukoski, E. E., "Turbulent Boundary-Layer Separation in Front of a Forward-Facing Step," *AIAA Journal*, Vol. 5, No. 10, 1967, pp. 1746–1753.

[32]Kim, K.-S., Lee, Y., Alvi, F. S., Settles, G. S., and Horstman, C. C., "Skin-Friction Measurements and Computational Comparison of Swept Shock/Boundary-Layer Interactions," *AIAA Journal*, Vol. 29, No. 10, 1991, pp. 1643–1650.

[33]Zheltovodov, A. A., "Properties of Two- and Three-Dimensional Separation Flows at Supersonic Velocities," *Izvestiya Akademii Nauk SSSR, Mekhanika Zhidkosti i Gaza*, Vol. 14, No. 3, 1979, pp. 42–50.

[34]Lu, F. K., and Settles, G. S., "Upstream-Influence Scaling of Sharp Fin Interactions," *AIAA Journal*, Vol. 29, No. 7, 1991, pp. 1180–1181.

[35]Hornung, H., "Regular and Mach Reflection of Shock Waves," *Annual Review of Fluid Mechanics*, Vol. 18, 1986, pp. 33–58.